Title: *HDAC1* overexpression alters GTPase activity impacting chemoresistance in pancreatic cancer

Authors: Carter A. Wright[1,2], Emily R. Gordon[2], Sara J. Cooper[2]

Affiliations:
[1]The University of Alabama in Huntsville, Huntsville, AL
[2]HudsonAlpha Institute for Biotechnology, Huntsville, AL

Abstract
Chromatin remodeling is a known mechanism of drug resistance in pancreatic ductal adenocarcinoma (PDAC). Here, we demonstrate that overexpression of *HDAC1*, a gene encoding a histone deacetylase involved in several chromatin remodeling complexes, is associated with multi-drug resistance and patient survival in PDAC. We characterized the effects of *HDAC1* overexpression in a pancreatic cancer cell line using transcriptomics and ChIP-sequencing for HDAC1 and H3K27 acetylation. These data showed that *HDAC1* overexpression results in a more stem-like state and contributes to chemoresistance in PDAC. We identified HDAC1 target genes and used them to develop a clinically relevant nine-transcript signature that predicts patient prognosis. One downstream consequence of *HDAC1* overexpression is GTPase activity, thus nominating GTPases as therapeutic drug targets with the potential to reverse chemoresistance. These findings nominate novel drug targets and propose a novel therapeutic tool to improve patient care.

Introduction
Pancreatic ductal adenocarcinoma (PDAC) is the most common form of pancreatic cancer and one of the most lethal cancers with a five-year survival rate of 11.5%. Due to the lack of early-stage symptoms, 52% of patients are diagnosed with unresectable, locally advanced, metastatic cancer[1]. Chemotherapeutics such as gemcitabine, abraxane, and combination therapies like FOLFIRINOX are standard of care treatments to improve prognosis, but chemoresistance develops in the majority of patients and contributes to the poor outcomes.

PDAC tumor cells achieve drug resistance through many cellular mechanisms. For example, over-activation of DNA damage repair processes limits the effectiveness of nucleoside analogs like gemcitabine. Tumors acquiring a mesenchymal phenotype, activated through genes involved in the epithelial to mesenchymal transition (EMT), become more invasive and have increased migratory potential[2]. Additionally, the hypovascular nature of PDAC tumors prevents sufficient delivery of oxygen to the tumor cells. This hypoxic environment promotes overexpression of anti-apoptotic genes (i.e. *Bcl-XL* and *FLIP*), suppressing apoptosis and contributing to drug resistance[2,3,4,]. Reduced blood flow also restricts delivery of drugs to tumors, further exacerbating resistance. Understanding mechanisms of drug resistance offers the potential for the development of therapeutic strategies that could reverse resistance or be less prone to the development of resistance.

Previous work, including our own publications linked chromatin remodeling genes to chemoresistance and patient survival in PDAC[5–7]. Chromatin remodeling is a mechanism of regulating gene expression through the rearrangement of chromatin structure which can alter DNA accessibility and influence transcription factor binding. This process can dramatically alter gene expression and lead to cellular reprogramming that contributes to chemoresistance. However, dysregulation of chromatin remodeling genes leads to global changes in gene expression making it

difficult to determine whether chromatin remodeling alters known resistance pathways, novel resistance pathways, or a combination[8].

We previously demonstrated that overexpression of *HDAC1* contributes to multidrug resistance in pancreatic cancer cells[9]. HDAC1 participates in several remodeling complexes including Sin3A, NuRD, and CoREST[10]. In cancer, HDAC1 regulates the acetylation of histone and non-histone proteins which modulate the expression of genes that influence cancer progression[8]. For example, HDAC1 is recruited along with the Sin3A complex to the promoter of *CDH1*, an epithelial cell marker, to deacetylate histones and silence *CDH1* expression during metastasis[8]. HDAC1 regulates expression of genes involved in apoptosis, DNA damage repair, metastasis, and EMT[8,11]. HDAC1 can also regulate tumor suppressors, such as CDKN1A (p21)[8].

While HDACs are canonically members of repressive complexes, several studies have identified circumstances under which binding of HDAC1 is associated with transcriptional activation[12,13]. In at least some cases, this is explained by HDAC1's ability to recruit RNA Pol II or regulate transcriptional elongation[12,13].

The ability of HDAC1 to regulate genes is important for drug resistance, cancer progression, and tumor suppression making it a strong candidate as a drug target. Several HDAC inhibitors (HDACi) have been tested (e.g. entinostat, romidepsin) for the treatment of both solid tumors and hematological malignancies[14]. However, clinical trials for HDACis in PDAC have been largely unsuccessful[14,15]. One likely reason for this is that inhibiting HDACs alters gene expression through the modification of histones, but also impacts the function of other non-histone proteins.
The observation that HDAC inhibition by commercially available HDACis leads to negative side effects in patients[16] is not surprising as HDACs have a broad impact on gene expression related to both cancer pathways and normal cellular functions; thus, inhibition of multiple HDACs using molecules that target a class of proteins causes global effects. Using genomic analyses of an *in vitro* system perturbing HDAC1 function, we identify genes and pathways regulated by HDAC1 which contribute to chemoresistance. Our study aims to identify HDAC1-regulated genes important for resistance that could be targeted by future drug development for the treatment of PDAC.

In this study, we overexpressed *HDAC1* in a well described PDAC cell line, MIA PaCa-2, and measured the effects on gene expression, HDAC1 binding, and chromatin structure to better understand how HDAC1 activation contributes to resistance. We found that HDAC1 overexpression leads to altered activity of pathways (e.g. EMT, resistance to apoptosis, altered cell cycle checkpoint, and increased hypoxia) that each have the potential to contribute to resistance. We show that *HDAC1* overexpression leads to a more mesenchymal phenotype *in vitro* and observe that *HDAC1* overexpression in patient tissues alters these pathways in a correlated way. Using ChIP-seq, we determined that the genes bound and regulated by HDAC1 were enriched for GTPases and their expression in patient tissues are negatively correlated with patient survival. We show that *HDAC1* overexpression results in altered expression of GTPases and thus increased GTPase activity suggesting that altered GTPase activity contributes to chemoresistance and represents possible targets to reverse resistance. Together these data reveal an improved mechanistic understanding of the role of HDAC1 in chemoresistance and nominate GTPase genes as potential therapeutic targets.

Results

HDAC1 overexpression leads to multi-drug resistance

HDAC1 expression has been previously linked to increased cellular resistance to cytotoxic chemotherapeutic drugs[9]. To further evaluate the effects of *HDAC1* overexpression on chemotherapeutic resistance, we used CRISPRa[17] to generate a stable MIA PaCa-2 cell line (MP2_HDAC1_OE) expressing *HDAC1* at ~3 times the levels of the levels of the control line (MP2_NTC) which expresses a non-targeting control guide (**Extended Data Fig. 1a**). We also treated the MIA PaCa-2 cell line with a HDAC1 siRNA to evaluate the effects of reducing *HDAC1* expression on chemoresistance (MP2_HDAC1_KD). We chose MIA PaCa-2 for our studies because it is a well-characterized line with modest to high expression of *HDAC1*. *HDAC1* is the most abundantly expressed HDAC gene in this line (**Extended Data Fig. 1b**). Under these three conditions, we measured the effect of treatment with irinotecan, gemcitabine, and oxaliplatin on cell viability (**Fig. 1a-c**). MP2_HDAC1_OE cells were more resistant to drug treatment than control cells and MP2_HDAC1_KD cells. Since *HDAC1* overexpression led to increased resistance to these drugs, we evaluated the effect of HDAC1 protein inhibition on drug response. We treated MP2_HDAC1_OE and MP2_NTC lines with romidepsin, a HDAC1/2 inhibitor, in combination with increasing concentrations of irinotecan. We observed a sensitizing effect of romidepsin on the MP2_HDAC1_OE cells treated with irinotecan (**Fig. 1d**). Together these experiments show a sensitizing effect of decreasing HDAC1 activity through either chemical inhibition or decreased expression.

HDAC1 overexpression is associated with markers of EMT in vitro and in human PDAC tissues

We performed RNA-sequencing to measure gene expression in MP2_HDAC1_OE and MP2_NTC cells. We found 1,259 genes that are differentially expressed with overexpression of *HDAC1* (padj < 0.1). These differentially expressed genes (DEG) were enriched for pathways involved in drug resistance: apoptosis, EMT, G2-M checkpoint, and hypoxia (**Fig. 2a, Extended Data Fig. 2**). Alteration of EMT-associated DEG can promote the transition to a more drug resistant mesenchymal cell state. As cells transition into a mesenchymal state their invasive and migratory properties are increased leading to therapeutic resistance[18]. For example, in PDAC cells, high levels of the cell surface marker CD44 is characteristic of the mesenchymal phenotype[19,20]. We detected a 1.8-fold increase in *CD44* expression upon overexpression of *HDAC1*. We used immunohistochemistry to examine the relative density of CD44 protein in PDAC cell lines and observed a comparable 2-fold increase in the MP2_HDAC1_OE cells compared to MP2_NTC cells **(Fig. 2b-c)** consistent with the expression data**.**

These data provide evidence that *HDAC1* overexpression modulates several known resistance pathways including EMT pathway in an *in vitro* model. Next, we sought to determine whether *HDAC1* overexpression in patient tumors leads to similar changes in gene expression. We used RNA-sequencing data collected from pancreatic tumor tissues from The Cancer Genome Atlas (TCGA) PDAC dataset. We grouped tissues based on their expression of *HDAC1* . We compared the lowest (n=45, $HDAC1^{HIGH}$) and highest (n=45, $HDAC1^{LOW}$) quartiles of *HDAC1* expressing samples to identify DEG in these tissues. We identified 10,592 DEG between $HDAC1^{HIGH}$ and $HDAC1^{LOW}$ tissues. We intersected this gene list with the 1,259 genes identified in our *in vitro* experiment and identified 322 genes that are significantly altered (padj < 0.1) in the same direction as we observed in cell lines. Heatmaps of the DEG in both datasets were clustered by sample which separated high and low *HDAC1* expression (**Fig. 3a,b**). These data indicate that there is a similar pattern of expression in the PDAC tissues as in the MP2_HDAC1_OE cells.

Given our previous finding that *HDAC1* overexpression can lead to *in vitro* drug resistance we wondered whether *HDAC1* expression might be associated with patient response to treatment. Our

best opportunity to capture treatment response is in information about patient prognosis. We hypothesized that genes associated with *HDAC1* overexpression might have prognostic value. We divided the 322 genes associated with increased *HDAC1* expression in both patient tissues and in the MP2_HDAC1_OE line between upregulated genes (n = 216) and downregulated (n = 106) genes. Across each gene set, we calculated an average gene expression value from TCGA PDAC patient tissues and compared the top and bottom quartiles in a survival analysis. We determined that overall survival was worse for patients with high expression of the upregulated genes and low expression of the downregulated genes (upregulated genes p = 0.00065, downregulated genes p = 0.0051, **Fig. 3c,d**). Although there are other possible interpretations, this finding is consistent with our observation that *HDAC1* overexpression is associated with drug resistance *in vitro* and supports the hypothesis that these genes might also impact drug response in patients and lead to decreased survival time. Importantly, overexpression of *HDAC1* alone only modestly predicts patient survival (p=0.44**, Extended Data Fig. 3**). Using an independent cohort (Kirby et al. 2016) we observed a similar difference in survival based on HDAC1-regulated genes (**Extended Data Fig. 4a,b**, upregulated genes p = 0.064, downregulated genes p = 0.19).

We compared the significance of the above signatures to other sets of genes that might be expected to be associated with patient outcomes. We compared prognostic predictions based on these 322 genes with the top 322 DEG in TCGA PDAC samples with high and low *HDAC1* expression as well as the top 322 DEG in our PDAC cell lines with *HDAC1* overexpression and controls. We observe that the top 322 DEG using either TCGA or cell line data data is less predictive than using genes associated with *HDAC1* overexpression in both tissues and cell lines (**Extended Data Fig. 5a,b**).

We used gene set enrichment analysis of the 322 DEG to identify sets of genes in this list that function together to better understand how these genes impact patient prognosis. This analysis revealed multiple cancer processes involved in drug resistance and progression including cadherin binding, cell-cell adhesion, regulation of cell migration, and GTPase activity (**Fig. 3e**, **Supplementary Table 1**). An example of a gene contributing to enrichment in GTPase activity is *RAP2B,* which we found was upregulated upon increased *HDAC1* expression (**Extended Data Fig. 6**). When activated, this GTPase promotes cell migration, cell adhesion, proliferation, and metastasis in cancer[21–23].

HDAC1 OE alters chromatin states in distal enhancer and promoter regions that regulate molecular switches

To identify direct and indirect impacts of *HDAC1* overexpression that might contribute to resistance, we measured genome-wide DNA binding of the HDAC1 protein and the presence of the activating histone mark, H3K27 acetylation (H3K27ac) using ChIP-sequencing in the MP2_HDAC1_OE and MP2_NTC cell lines. Using the standard ENCODE ChIP-seq protocol for peak calling[24], we identified 17,457 binding sites for HDAC1 (10,033 unique to MP2_HDAC1_OE). We found 30,961 regions of H3K27ac; 8,392 were unique to MP2_HDAC1_OE and 5,916 were unique to MP2_NTC (**Fig. 4a**). We observed an enrichment of HDAC1 binding and regions of H3K27ac near the transcription start sites (TSS) of DEG when *HDAC1* is overexpressed. The H3K27ac peaks specific to *HDAC1* overexpressing cells occurred significantly more near the upregulated genes despite HDAC1's canonical role as a repressor (**Extended Data Fig. 7**).

HDAC1 overexpression quantitatively changes chromatin structure as measured by increasing or decreasing signals for HDAC1 binding and H3K27 acetylation. H3K27ac and HDAC1 peaks were called and a region 500 bp upstream and downstream of the peak center was defined. Searching

within 2kb of the TSS for all DEG, we identified 1,857 regions nearby 1,040 DEG that had at least one HDAC1 or H3K27ac peak. Gene set enrichment analysis of these 1,040 DEG revealed enrichment for GTPase activity, cadherin binding, and DNA binding (FDR < 0.05) (**Supplementary Table 2**).

To better understand how *HDAC1* overexpression impacts H3K27ac and influences gene expression, we divided regions of HDAC1 binding and H3K27 acetylation based on whether they were increasing or decreasing across a region. Using the sequencing reads collected in a region called as a peak in any of our ChIP-seq experiments, we calculated a fold-change to determine whether there was evidence of increased or decreased binding. Given HDAC1's canonical role as a repressor, we would expect that increased HDAC1 binding would be associated with decreased H3K27 acetylation, however, we only identified 235 DEG with increased HDAC1 binding and reduced H3K27 acetylation in the promoter regions (+/- 2kb from TSS). On the contrary, 597 DEG had increased HDAC1 binding and increased H3K27 acetylation (fold-change > 1) in their promoter regions upon *HDAC1* overexpression (**Supplementary Table 3**). Since previous studies have shown that HDAC1 is more abundant near active genes[13], we tested if high expression of DEG with altered HDAC1 binding and H3K27 acetylation are associated with worse overall patient survival. We performed survival analysis comparing outcomes of patients with the top 25% and bottom 25% average tumor gene expression of these 597 genes. Patients with the highest average gene expression of upregulated genes and lowest average gene expression of downregulated genes have worse overall survival (upregulated: p = 0.0021, **Fig. 4b,** downregulated: p = 0.023, **Extended Data Fig. 8a**). We also showed that *HDAC1* expression is significantly higher in patients with the top 25% of average tumor gene expression of the 597 genes (**Extended Data Fig. 8b**).

A nine-gene signature of HDAC1 regulated genes predicts PDAC patient survival

Identification of prognostic signatures associated in PDAC could be of clinical utility. The analyses above identified a set of 597 genes, regulated by HDAC1 that can predict patient outcomes based on *in vitro* and *in vivo* signatures of *HDAC1* overexpression in the TCGA cohort, although expression of *HDAC1* alone is not prognostic. A simplified signature of patient prognosis was developed using a multivariate logistic regression with L1 penalized log partial likelihood (LASSO) for feature selection[25]. From the 597 genes, LASSO identified a 9-transcript model sufficient to differentiate TCGA PDAC tumors with high and low *HDAC1* expression (**Extended Data Fig. 8c,d**). To determine the clinical relevance of the genes selected using the LASSO model, survival analysis was performed using the patients in the top and bottom quartile of predictor values from the regression and those with the highest predictor values had worse overall survival (**Fig. 4e**, p = 0.037). Interestingly, though it represents only 11 individuals, patients with the lowest 25% of predictor values show higher survival rates.

***HDAC1* overexpression leads to increased GTPase activity and chemoresistance**

The identification of many DEG upon *HDAC1* overexpression led us to explore some pathways that have not been previously linked to chemoresistance. Pathway enrichment analysis of DEG with increased HDAC1 binding and H3K27 promoter acetylation (n = 597) identified an enrichment for many known cancer pathways (**Supplementary Table 4**). Included on this list was Ras signaling, regulation of apoptotic signaling pathway, chromatin binding, and GTPase activity. GTPase activity was also significant in enrichment analyses driven by overexpression of the GTPases and associated proteins (e.g. *RALB*, *RAB27B*, and *RAC1)* which have increased expression with *HDAC1* overexpression. ARHGAP5, a Rho family-GTPase activating protein (**Fig. 5a**), was also increased with *HDAC1* overexpression and we observed increased HDAC1 binding and H3K27 acetylation near its TSS (**Fig. 5b**). Since activation of GTPase activity is not a well described

mechanism of drug resistance, we used existing data to search for additional evidence that GTPase activity, as measured by the expression of GTPase genes might impact cellular response to drugs. We used RNA-sequencing data from 14 unmodified PDAC cells lines with varying response to gemcitabine (Data from Kirby 2016) and found that cell lines with increased expression of genes influencing GTPase activity had higher levels of resistance to gemcitabine (**Fig. 5c**). We identified a total of 11 genes that modulate GTPase activity and they all show a similar pattern of expression in resistant lines (**Extended Data Fig. 9).** Increased GTPase activity activates the MAPK and PI3K pathways which promote proliferation and survival in cancer[26]. KEGG[27] pathway mapping of these 597 DEG confirmed the increased expression of genes in the MAPK and PI3K pathways upon *HDAC1* overexpression (**Extended Data Fig. 10a,b**).

Given the increase in transcript levels of several GTPases (**Fig 5d**), we tested whether there was a measurable difference in GTPase activity upon HDAC1 overexpression. GTPase activity was measured through the detection of GTP remaining after a GTP hydrolysis reaction catalyzed by cell lysates from the MP2_HDAC1_OE line compared to the MP2_NTC line. Measurement of GTPase activity revealed that MP2_HDAC1_OE cell lysates have increased GTPase activity (**Fig. 5e**). MP2_HDAC1_OE cells had the highest GTPase activity and treatment of MIA PaCa-2 cells with romidepsin, a HDAC1/2 inhibitor, led to decreased GTPase activity ($p < 0.05$) (**Supplementary Table 5**).

Methods

Cell Culture

MiaPaCa-2 cells (ATCC #CRM-CRL-1420) were cultured in D10 media: DMEM (Lonza #12-614Q) supplemented with 10% FBS (GELifeSciences #SH30071.03), and 0.5% penicillin-streptomycin (ThermoFisher #15140122). All cell lines were maintained at 37 °C and 5% CO2. Cells were cryopreserved with the addition of 10% DMSO (EMD #MX1458-6).

Plasmids

LentiCRISPRv2 (Addgene #52961) or lentiSAMv2 (Addgene #92062) and lenti-MS2-p65-HSF1-Hygro (Addgene #89308) were used to generate stable cell lines for gene knockout and activation, respectively. pMD2.G (Addgene #12259) and psPAX2 (Addgene #12260) were used to facilitate viral packaging of sgRNA pools and single vector plasmids.

sgRNA Cloning

gRNA oligos were designed and cloned into their respective plasmids as described previously[17].

DsiRNA

IDT TriFECTa RNAi kit was used per manufacturer's protocol. 100,000 cells were seeded in 1 well of a 12 well tissue culture treated plate 24 hours prior to transfection. Cells were transfected using RNAiMax (ThermoFisher #13778-030) following manufacturer's recommended protocol. As indicated in the TriFecta kit (IDT #hs.Ri.HDAC1.13), TYE 563 transfection efficiency control, positive HPRT-S1 control, and negative (DS NC1) scrambled sequence control were utilized. Further assays were performed 48 hours after transfection. Expression was validated with each transfection with the IDT PrimeTime qPCR Assay system on an Agilent QuantStudio 6 Flex Real-Time PCR system.

DsiRNA Sequences:

IDT DsiRNA name	DsiRNA Sequence
hs.Ri.HDAC1.13.1-SEQ1	rArGrUrUrUrCrCrUrUrUrUrUrGrArGrArUrArCrUrArUrUTT
hs.Ri.HDAC1.13.1-SEQ2	rArArArArUrArGrUrArUrCrUrCrArArArArArGrGrArArArCrUrArG

hs.Ri.HDAC1.13.2-SEQ1	rCrUrGrGrArArCrUrGrCrUrArArArGrUrArUrCrArCrCrAGA
hs.Ri.HDAC1.13.2-SEQ2	rUrCrUrGrGrUrGrArUrArCrUrUrUrArGrCrArGrUrUrCrCrArGrGrA
hs.Ri.HDAC1.13.3-SEQ1	rArGrCrCrGrGrUrCrArUrGrUrCrCrArArArGrUrArArUrGGA
hs.Ri.HDAC1.13.3-SEQ2	rUrCrCrArUrUrArCrUrUrUrGrGrArCrArUrGrArCrCrGrGrCrUrUrG

qPCR Sequence IDs:

Gene	Exon	IDT primeTime Assay ID
HDAC1	1-2	Hs.PT.58.20534173
HDAC1	3-4	Hs.PT.58.38680914
ACTB	1-2	Hs.PT.39a.22214847
GAPDH	2-3	Hs.PT.39a.22214836
HPRT1	8-9	Hs.PT.58v.45621572

GTPase-Glo Assay Using Cell Lysates

In vitro GTPase activity was measured using the GTPase-Glo assay (Promega #V7681). We followed the protocol as described[28] with modifications for use of cell lysates. Cell lysates were made from the following cell lines: MIA PaCa-2, MP2_HDAC1_OE, MP2_NTC, and MIA PaCa-2 treated with 0.01 μM romidepsin, an HDAC1 inhibitor. Cells (2 x 10^6 per tube) were lysed in a lysis buffer containing 50 mM HEPES at pH 7.6, 150 mM NaCl, 10% Glycerol, 0.1% NP-40, and 2 mM $MgCl_2$. To generate the lysate, 10μL of lysis buffer per 100,000 cells was added to each cell pellet and resuspended. Lysates were mixed for 30 minutes at 4°C, vortexed in three 10 second intervals, then centrifuged at 4°C for 30 minutes at 16.1x RCF. A 2X GTP solution was prepared and the reaction was initiated following the manufacturer's protocol.

Modifications for cell lysates required background wells for each cell line. GTPase-Glo Buffer was added to cell lysates at a final concentration of 1 μL per 10,000 cells. After the GTPase reaction, 20μL was added to each respective background well. Luminescence was measured using a BioTek Synergy H5 plate reader. To calculate GTPase activity for each cell type, we calculated the difference between the luminescence of the experimental wells and background wells. GraphPad Prism 9 (version 9.3.1) was used for plotting bar charts and t-tests performed in GraphPad were unpaired, parametric, two-tailed with 95% confidence interval.

ChIP-sequencing

MP2_HDAC1_OE and MP2_NTC cells (2 x 10^7) were cross-linked, harvested, and DNA was precipitated using a commercial H3K27ac antibody (Abcam, ab4729). Libraries were constructed, pooled, and sequenced using an Illumina NovaSeq instrument with 75bp single-end reads. These data were generated and analyzed using published ENCODE protocols (https://www.encodeproject.org/documents/).

Differential binding analysis was conducted using the "multiBigwigSummary" tool from the "deepTools" package[29]. Using this tool, a ChIP-seq score was generated for each sample and region using genomic coordinates defined as +/- 500 bp from the center of peaks defined using the

published ENCODE protocol[24] and 1 kb upstream of all annotated genes. Regions were merged together if they overlapped. We omitted any regions with a ChIP-seq score less than 1 for both MP2_HDAC1_OE and MP2_HDAC1_NTC. Using the ChIP-seq score, we calculated a fold-change between MP2_HDAC1_OE and MP2_NTC for HDAC1 and H3K27ac in each defined region. The criteria for differentially bound regions was a fold-change greater than or less than one for HDAC1 binding and H3K27 acetylation.

3' RNA-sequencing

Cell pellets were frozen at -80°C until RNA extraction. For RNA extraction 350 µl of RL Buffer plus 1% β-ME from the Norgen Total RNA extraction kit was added to each cell pellet and extraction proceeded per manufacturer's instructions including use of the DNase kit (Norgen # 37500, 25720). RNA quality was verified with the Agilent BioAnalyzer RNA Nano 600 kit (cat# 5067-1512) with the RIN range between 9.2-10. RNA-sequencing libraries were made using Lexogen QuantSeq 3' mRNA-Seq Library Prep Kit FWD for Illumina kit (cat# 015.24) with 250 ng of RNA input. They were pooled and sequenced on an Illumina NextSeq 500 instrument with 75 bp single-end reads. Read counts averaged 4 million reads and an average Q30 of 91.28%. Lexogen's BlueBee integrated QuantSeq data analysis pipeline was used for trimming, mapping, and alignment and the R package "DESeq2" was used for differential expression analysis.

Drug resistance screening

Cells were seeded in 96-well plates at 2000 cells/well. Seeded cells were dosed with a range of gemcitabine, oxaliplatin, or irinotecan concentrations. Cells were re-dosed 48 hours later. The number of viable cells surviving drug treatment were assayed with CellTiter-Glo (Promega #G7571) 24 hours after the last drug treatment per manufacturer's protocol using a BioTek Synergy H5 plate reader.

HDAC1 inhibition with romidepsin (Sigma #SML1175-1MG) was performed similarly to above except that cells were dosed every 24 hours with either 0.01 µM romidepsin, a range of gemcitabine, or both. Equal volume DMSO was used as a control in place of romidepsin. The number of viable cells surviving drug treatments were assayed with CellTiter-Glo (Promega #G7571) 24 hours after the last drug treatment per manufacturer's protocol using a BioTek Synergy H5 plate reader. In both cases, data were plotted using GraphPad Prism 9, version 9.3.1. T-tests performed were unpaired, parametric, two-tailed with 95% confidence interval.

Cell staining

75,000 MIA PaCa-2 cells with non-targeting, HDAC1 OE sgRNAs, or HDAC1 KD with DsiRNA were seeded in 12 well plates. Cells were stained using Alexa Fluor 488 Conjugate kit for live cell imaging (LifeTechnologies #A25618) for CD44 via the manufacturer's protocol. DAPI (Invitrogen #D21490) was counterstained per manufacturer's protocols for adherent cells. Presence of CD44 in the cells was quantified using ImageJ 1.53K with measurements (area, mean, and integrated density) for stain and background taken with the freehand selection tool. Relative CD44 intensity or bound CD44 per area was calculated for each cell by: integrated density of cell-integrated density of background for that cell/area of that cell. GraphPad Prism 9 (version 9.3.1) was used for plotting violin plots and t-tests performed in GraphPad were unpaired, parametric, two-tailed with 95% confidence interval.

Enrichment Analysis

Enrichr, a comprehensive gene set analysis web server, and the R package "ClusterProfiler" (version 3.12.0)[30] were used for enrichment analysis of the differentially expressed genes[31]. We

focused on the pathways (MSigDB) and gene ontology terms (GO MF, GO BP) reaching the significance threshold of FDR < 0.05.

Survival Analysis

To conduct survival analysis, clinical and RNAseq expression data was retrieved from The Cancer Genome Atlas (TCGA) for 178 PDAC (TCGA-PAAD) patients (https://portal.gdc.cancer.gov/). Data was normalized using the R package "DESeq2"[32] and differentially expressed genes with an FDR < 0.1 were used to generate Kaplan-Meier survival curves. We classified tissues based on their average expression of a given gene set (bottom, middle, and top quartiles of gene expression). We compared the patients with the lowest and highest quartile of average gene expression and performed survival analysis. Survival curves and analyses were generated using the "ggplot2", "survminer", and "survival" R packages[33–35].

Clinical Data and Samples

Clinical data and RNA-sequencing data for TCGA-PAAD samples were retrieved on 04/01/2020 using the GDC Data Portal. Our analyses included 178 samples in this cohort that had matched clinical and RNA-sequencing data.

Data Access

ChIP-sequencing data is available using the GEO accessions GSE209895 (H3K27ac) and GSE158541 (HDAC1).

RNA-sequencing is available using the GEO accessions GSE79668 (Kirby, et.al tumor data) and GSE79669 (gemcitabine resistant and sensitive cell lines).

Statistical Testing

Statistical analysis was conducted in R (version 1.2.1335). The following R packages and software were used for analysis:
survival (version 1.2.1335)[34]
survminer (version 0.4.9)[35]
ggplot2 (version 3.3.6)[33]
DESeq2 (version 1.24.0)[32]
pheatmap (version 1.0.12)[36]
clusterProfiler (version 3.12.0)[30]
glmnet (version 4.1-3)[37]
ROCR (version 1.0-11)[38]
deepTools (version 3.5.0)[29]
IGV (version 2.7.2)[39]

LASSO model selection

A predictive gene signature from transcripts that are differentially expressed (DESeq2 FDR < 0.1) and have increased HDAC1 binding and H3K27 acetylation near their TSS (+/- 2000 bp) was developed using the LASSO regression model. LASSO was performed using the R package "glmnet" (version 4.1-3)[37]. The TCGA PDAC cohort was split into three groups by *HDAC1* expression (top 25%, middle 50%, and bottom 25%). The cohort was further subsetted by randomly distributing an equal number of samples from the top 25% and bottom 25% of *HDAC1* expression into two groups (n = 45). The training cohort and the validation cohort used the same dichotomization threshold (top 25% and bottom 25% of *HDAC1* expression). Model performance was evaluated based on the model's ability to classify patients into the high or low *HDAC1*

expression group. We generated an area under the curve (AUC) value using the R package "ROCR" (version 1.0-11)[38]. Kaplan-Meier curves were generated using the R package "survival" (version 3.2-13)[34].

Data Analysis

The adjusted p-value was used to determine the top 322 differentially expressed genes in TCGA PDAC samples for comparison of patients in the top and bottom quartile of *HDAC1* expression. Using the R package "DESeq2" (version 1.24.0)[32], differentially expressed genes were excluded from the analysis if baseMean < 10.

Discussion

Pancreatic cancer has ranked among the deadliest cancers for decades due to its chemoresistant nature and insufficient treatment options. Understanding what drives chemoresistance is essential to identifying new therapeutic targets and improving patient outcomes. Chromatin remodeling has been established as a critical feature of tumorigenesis and cancer progression, making the pathway an attractive drug target. Our work and others showing the importance of key genes like *HDAC1* in chemoresistance have nominated chromatin remodeling genes as possible drug targets. Using a combination of genomic and biochemical approaches we revealed potential mechanisms by which *HDAC1* OE contributes to chemoresistance and showed that HDAC1 inhibition sensitizes PDAC cells to chemotherapeutic treatment further strengthening the argument that this pathway is a good candidate for treatment, however HDAC inhibitors have faced challenges in clinical trials. Commercial HDAC inhibitors target a class of HDACs and not specific proteins. This decreased specificity leads to genome-wide off target effects and patient toxicity. That has motivated the current study which aims to better understand how *HDAC1* activation contributes to resistance and reveal novel downstream targets that may lead to alternative treatment strategies.

In contrast to other tumor types, multiple large scale drug trials that used targeted therapy were not successful in pancreatic cancer[40,41], thus using a targeted gene panel that can be used to better define potential treatment options for PDAC patients could lead to improved survival and quality of life[42,43]. In this study, we collected data from an *in vitro* system testing the impact of *HDAC1* overexpression on PDAC cells and combined these results with information from publicly available gene expression data gathered from both tissues of PDAC patients and PDAC cell lines to show that *HDAC1* overexpression regulates a set of transcriptomic responses that contribute to chemoresistance and the genes regulated by HDAC1 can also be shown to predict patient outcome. *HDAC1* overexpression alone is not significantly prognostic of worse overall survival in PDAC patients. Conversely, the genes altered by *HDAC1* overexpression are prognostic. Since HDAC1 is a genome-wide regulator of gene expression, in PDAC, we hypothesize that the genes contributing to a worse overall survival prognosis, resulting from tumorigenesis and drug resistance, are the subset of genes altered by *HDAC1* overexpression. These results show that pathways under the control of HDAC1 contribute to patient outcomes and could be used to predict outcomes that may be linked to treatment response. Of the 597 genes altered by *HDAC1* expression *in vitro*, we identified a 9-transcript novel signature that successfully predicted patients with high and low *HDAC1* expression and was correlated with patient survival. These analyses provided insight into a subset of genes that are regulated by HDAC1 and are predictive of worse patient survival, suggesting a potential clinical utility. Our panel of biomarkers represents a potential step forward in the development of an assay that is predictive of patient survival which could influence treatment decisions.

We integrated several datasets to better understand how *HDAC1* overexpression impacts PDAC cells. These studies revealed several processes known for their role in tumorigenesis, progression and drug resistance. One of these was EMT. In addition to its role in progression, EMT is associated with suppression of proteins involved in drug transport, such as CNT3, allowing the cells to evade the anti proliferative effects of chemotherapeutics (gemcitabine)[44]. Cells that undergo EMT also have a more stem cell-like phenotype making them more resistant to chemotherapeutics[2]. Increased expression of *CD44*, a cell surface protein important for cell adhesion and migration, is associated with a more mesenchymal-like phenotype which is characteristic of EMT[19]. This is in agreement with our finding that CD44 transcript and protein are more abundant in cells with *HDAC1* overexpression and our past work showing that *HDAC1* OE leads to increased migration[9].

Induction of EMT is also associated with drug resistance and we showed that MP2_HDAC1_OE cells are resistant to multiple drugs suggesting a regulatory role for HDAC1 in drug resistance. Understanding the direct impacts of HDAC1 binding and H3K27ac occupancy is necessary to determine the effects of *HDAC1* overexpression in pancreatic cancer. Our ChIP-seq experiments revealed altered H3K27 acetylation and HDAC1 binding near HDAC1 regulated genes. Interestingly, we found that the majority of the DEG with HDAC1 binding had an increase in both HDAC1 and H3K27ac occupancy near their promoter. Our findings are in agreement with a previously published study concluding that HDAC1 binding is enriched at actively transcribed genes[13]. Despite current efforts, it is still not well understood how HDAC1 binding directly affects the activation of gene expression. Greer et al. did show that HDAC1 binding can regulate RNA Pol II recruitment and that HDAC1 may regulate transcription elongation through interaction with BRD4. Additionally, HDAC1 is known to deacetylate proteins other than histones which might facilitate activation of nearby transcription factors (e.g. MYC)[12].

Throughout this study, our gene set enrichment analyses of genes associated with *HDAC1* overexpression consistently revealed GTPase activity as an enriched process. A variety of proteins contribute to GTPase activity and many are druggable[45], which makes them of potential clinical interest. We have shown that expression of GTPases and GTPase activating proteins are associated with worse overall survival in patients with increased *HDAC1* expression. We used biochemical assays to confirm that MP2_HDAC1_OE cells have higher GTPase activity than control cells and that cells treated with a HDACi have further reduced GTPase activity. GTPase signaling is involved in pancreatic cancer initiation, metastasis, and drug resistance[46]. Increased GTPase signaling leads to the activation of key pathways, such as MAPK and PI3K, that regulate cell proliferation, migration, and survival in cancer[26]. We have shown that the expression of genes in the MAPK and PI3K pathways are increased upon *HDAC*1 overexpression highlighting one known pathway altered by HDAC1 that contributes to PDAC progression[47]. GTPases, such as RAC1, have been shown to activate EMT pathway in multiple cancers, thus leading to a more invasive and drug resistant phenotype[48–50] and we show that *RAC1* expression is increased upon *HDAC1* overexpression in PDAC cells. Additionally, ARHGAP5, is a GTPase activating protein associated with promoting EMT, a known mechanism of drug resistance in colorectal cancer, but its role in PDAC is not well understood[51]. We showed that expression of *ARHGAP5* and of several other proteins promoting GTPase activity are increased upon *HDAC1* overexpression and their transcripts are more abundant in gemcitabine resistant PDAC cell lines.

Despite decades of research, PDAC patients continue to have limited treatment options and suffer poor outcomes. Identifying patients who will benefit most from existing options compared to those who could benefit from an alternative treatment is a key clinical need. Our work identified sets of genes that may help identify patients with poor prognosis due at least in part to treatment

resistance. These patients are in need of new therapeutic targets. Our study identifies a novel set of genes relevant for predicting patient outcomes while also nominating potential novel drug targets for patients not likely to respond to existing treatments.

References

1. Cancer of the pancreas - cancer stat facts. *SEER* https://seer.cancer.gov/statfacts/html/pancreas.html.
2. Palamaris, K., Felekouras, E. & Sakellariou, S. Epithelial to Mesenchymal Transition: Key Regulator of Pancreatic Ductal Adenocarcinoma Progression and Chemoresistance. *Cancers* **13**, (2021).
3. Shah, V. M., Sheppard, B. C., Sears, R. C. & Alani, A. W. Hypoxia: Friend or Foe for drug delivery in Pancreatic Cancer. *Cancer Lett.* **492**, 63–70 (2020).
4. Beatty, G. L., Werba, G., Lyssiotis, C. A. & Simeone, D. M. The biological underpinnings of therapeutic resistance in pancreatic cancer. *Genes Dev.* **35**, 940–962 (2021).
5. Hasan, N. & Ahuja, N. The Emerging Roles of ATP-Dependent Chromatin Remodeling Complexes in Pancreatic Cancer. *Cancers* **11**, (2019).
6. Ying, H. *et al.* Genetics and biology of pancreatic ductal adenocarcinoma. *Genes Dev.* **30**, 355–385 (2016).
7. McCleary-Wheeler, A. L. *et al.* Insights into the epigenetic mechanisms controlling pancreatic carcinogenesis. *Cancer Lett.* **328**, 212–221 (2013).
8. Li, Y. & Seto, E. HDACs and HDAC Inhibitors in Cancer Development and Therapy. *Cold Spring Harb. Perspect. Med.* **6**, (2016).
9. Ramaker, R. C. *et al.* Pooled CRISPR screening in pancreatic cancer cells implicates co-repressor complexes as a cause of multiple drug resistance via regulation of epithelial-to-mesenchymal transition. *BMC Cancer* vol. 21 (2021).
10. Park, S.-Y. & Kim, J.-S. A short guide to histone deacetylases including recent progress on class II enzymes. *Exp. Mol. Med.* **52**, 204–212 (2020).
11. Hai, R., He, L., Shu, G. & Yin, G. Characterization of Histone Deacetylase Mechanisms in Cancer Development. *Front. Oncol.* **11**, 700947 (2021).
12. Greer, C. B. *et al.* Histone Deacetylases Positively Regulate Transcription through the

Elongation Machinery. *Cell Rep.* **13**, 1444–1455 (2015).

13. Wang, Z. *et al.* Genome-wide mapping of HATs and HDACs reveals distinct functions in active and inactive genes. *Cell* **138**, 1019–1031 (2009).
14. Koutsounas, I., Giaginis, C. & Theocharis, S. Histone deacetylase inhibitors and pancreatic cancer: are there any promising clinical trials? *World J. Gastroenterol.* **19**, 1173–1181 (2013).
15. Hontecillas-Prieto, L. *et al.* Synergistic Enhancement of Cancer Therapy Using HDAC Inhibitors: Opportunity for Clinical Trials. *Front. Genet.* **11**, 578011 (2020).
16. Laschanzky, R. S. *et al.* Selective Inhibition of Histone Deacetylases 1/2/6 in Combination with Gemcitabine: A Promising Combination for Pancreatic Cancer Therapy. *Cancers* **11**, (2019).
17. Joung, J. *et al.* Genome-scale CRISPR-Cas9 knockout and transcriptional activation screening. *Nat. Protoc.* **12**, 828–863 (2017).
18. Bulle, A. & Lim, K.-H. Beyond just a tight fortress: contribution of stroma to epithelial-mesenchymal transition in pancreatic cancer. *Signal Transduct Target Ther* **5**, 249 (2020).
19. Zhao, S. *et al.* CD44 Expression Level and Isoform Contributes to Pancreatic Cancer Cell Plasticity, Invasiveness, and Response to Therapy. *Clin. Cancer Res.* **22**, 5592–5604 (2016).
20. Luu, T. Epithelial-Mesenchymal Transition and Its Regulation Mechanisms in Pancreatic Cancer. *Front. Oncol.* **11**, 646399 (2021).
21. Li, J. *et al.* TMEM43 promotes pancreatic cancer progression by stabilizing PRPF3 and regulating RAP2B/ERK axis. *Cell. Mol. Biol. Lett.* **27**, 24 (2022).
22. Miao, F. *et al.* Rap2B promotes cell adhesion, proliferation, migration and invasion of human glioma. *J. Neurooncol.* **143**, 221–229 (2019).
23. Di, J. *et al.* Rap2B promotes proliferation, migration, and invasion of human breast cancer through calcium-related ERK1/2 signaling pathway. *Sci. Rep.* **5**, 12363 (2015).
24. Landt, S. G. *et al.* ChIP-seq guidelines and practices of the ENCODE and modENCODE consortia. *Genome Res.* **22**, 1813–1831 (2012).
25. Tibshirani, R. Regression shrinkage and selection via the lasso. *J. R. Stat. Soc.* **58**, 267–288 (1996).

26. Soriano, O., Alcón-Pérez, M., Vicente-Manzanares, M. & Castellano, E. The Crossroads between RAS and RHO Signaling Pathways in Cellular Transformation, Motility and Contraction. *Genes* **12**, (2021).
27. Kanehisa, M., Furumichi, M., Sato, Y., Ishiguro-Watanabe, M. & Tanabe, M. KEGG: integrating viruses and cellular organisms. *Nucleic Acids Res.* **49**, D545–D551 (2021).
28. Mondal, S., Hsiao, K. & Goueli, S. A. A Homogenous Bioluminescent System for Measuring GTPase, GTPase Activating Protein, and Guanine Nucleotide Exchange Factor Activities. *Assay Drug Dev. Technol.* **13**, 444–455 (2015).
29. Ramírez, F., Dündar, F., Diehl, S., Grüning, B. A. & Manke, T. deepTools: a flexible platform for exploring deep-sequencing data. *Nucleic Acids Res.* **42**, W187–91 (2014).
30. Yu, G., Wang, L.-G., Han, Y. & He, Q.-Y. clusterProfiler: an R package for comparing biological themes among gene clusters. *OMICS* **16**, 284–287 (2012).
31. Chen, E. Y. *et al.* Enrichr: interactive and collaborative HTML5 gene list enrichment analysis tool. *BMC Bioinformatics* **14**, 128 (2013).
32. Love, M. I., Huber, W. & Anders, S. Moderated estimation of fold change and dispersion for RNA-seq data with DESeq2. *Genome Biol.* **15**, 550 (2014).
33. Wickham, H. *ggplot2: Elegant Graphics for Data Analysis*. (Springer International Publishing, 2016).
34. The survival package in R. *Design of Experiments for Reliability Achievement* 339–350 (2022) doi:10.1002/9781119237754.app1.
35. Kassambara, Kosinski, Biecek & Fabian. survminer: Drawing Survival Curves using ‘ggplot2’. *R package version 0.3*.
36. pheatmap: Pretty Heatmaps. *Comprehensive R Archive Network (CRAN)* https://cran.r-project.org/web/packages/pheatmap/index.html.
37. Hastie, T., Qian, J. & Tay, K. An Introduction to glmnet. *CRAN R Repositary* (2021).
38. Sing, T., Sander, O., Beerenwinkel, N. & Lengauer, T. ROCR: visualizing classifier performance in R. *Bioinformatics* **21**, 3940–3941 (2005).
39. Thorvaldsdottir, H., Robinson, J. T. & Mesirov, J. P. Integrative Genomics Viewer (IGV):

high-performance genomics data visualization and exploration. *Briefings in Bioinformatics* vol. 14 178–192 (2013).

40. Hecht, J. R. *et al.* Randomized Phase III Study of FOLFOX Alone or With Pegilodecakin as Second-Line Therapy in Patients With Metastatic Pancreatic Cancer That Progressed After Gemcitabine (SEQUOIA). *J. Clin. Oncol.* **39**, 1108–1118 (2021).
41. Tempero, M. *et al.* Ibrutinib in combination with nab-paclitaxel and gemcitabine for first-line treatment of patients with metastatic pancreatic adenocarcinoma: phase III RESOLVE study. *Ann. Oncol.* **32**, 600–608 (2021).
42. Hosein, A. N., Dougan, S. K., Aguirre, A. J. & Maitra, A. Translational advances in pancreatic ductal adenocarcinoma therapy. *Nat Cancer* **3**, 272–286 (2022).
43. Wei, X. *et al.* A 14-gene gemcitabine resistance gene signature is significantly associated with the prognosis of pancreatic cancer patients. *Sci. Rep.* **11**, 6087 (2021).
44. Zheng, X. *et al.* Epithelial-to-mesenchymal transition is dispensable for metastasis but induces chemoresistance in pancreatic cancer. *Nature* **527**, 525–530 (2015).
45. Prieto-Dominguez, N., Parnell, C. & Teng, Y. Drugging the Small GTPase Pathways in Cancer Treatment: Promises and Challenges. *Cells* **8**, (2019).
46. Yoshimachi, S. *et al.* Ral GTPase-activating protein regulates the malignancy of pancreatic ductal adenocarcinoma. *Cancer Sci.* **112**, 3064–3073 (2021).
47. Mehra, S., Deshpande, N. & Nagathihalli, N. Targeting PI3K Pathway in Pancreatic Ductal Adenocarcinoma: Rationale and Progress. *Cancers* **13**, (2021).
48. Fang, D. *et al.* Epithelial-mesenchymal transition of ovarian cancer cells is sustained by Rac1 through simultaneous activation of MEK1/2 and Src signaling pathways. *Oncogene* **36**, 1546–1558 (2017).
49. Zhou, Y. *et al.* Rac1 overexpression is correlated with epithelial mesenchymal transition and predicts poor prognosis in non-small cell lung cancer. *J. Cancer* **7**, 2100–2109 (2016).
50. Ungefroren, H., Witte, D. & Lehnert, H. The role of small GTPases of the Rho/Rac family in TGF-β-induced EMT and cell motility in cancer. *Developmental Dynamics* vol. 247 451–461 (2018).

51. Tian, T. *et al.* Investigation of the role and mechanism of ARHGAP5-mediated colorectal cancer metastasis. *Theranostics* **10**, 5998–6010 (2020).

Acknowledgements
We thank the Myers and Cooper labs for helpful feedback. We also acknowledge The Cancer Genome Atlas which were extremely valuable and without which this study would not be possible. SJC is supported by UL1TR003096. SJC, ERG, and CAW are supported by Alabama's State Cancer Fund.

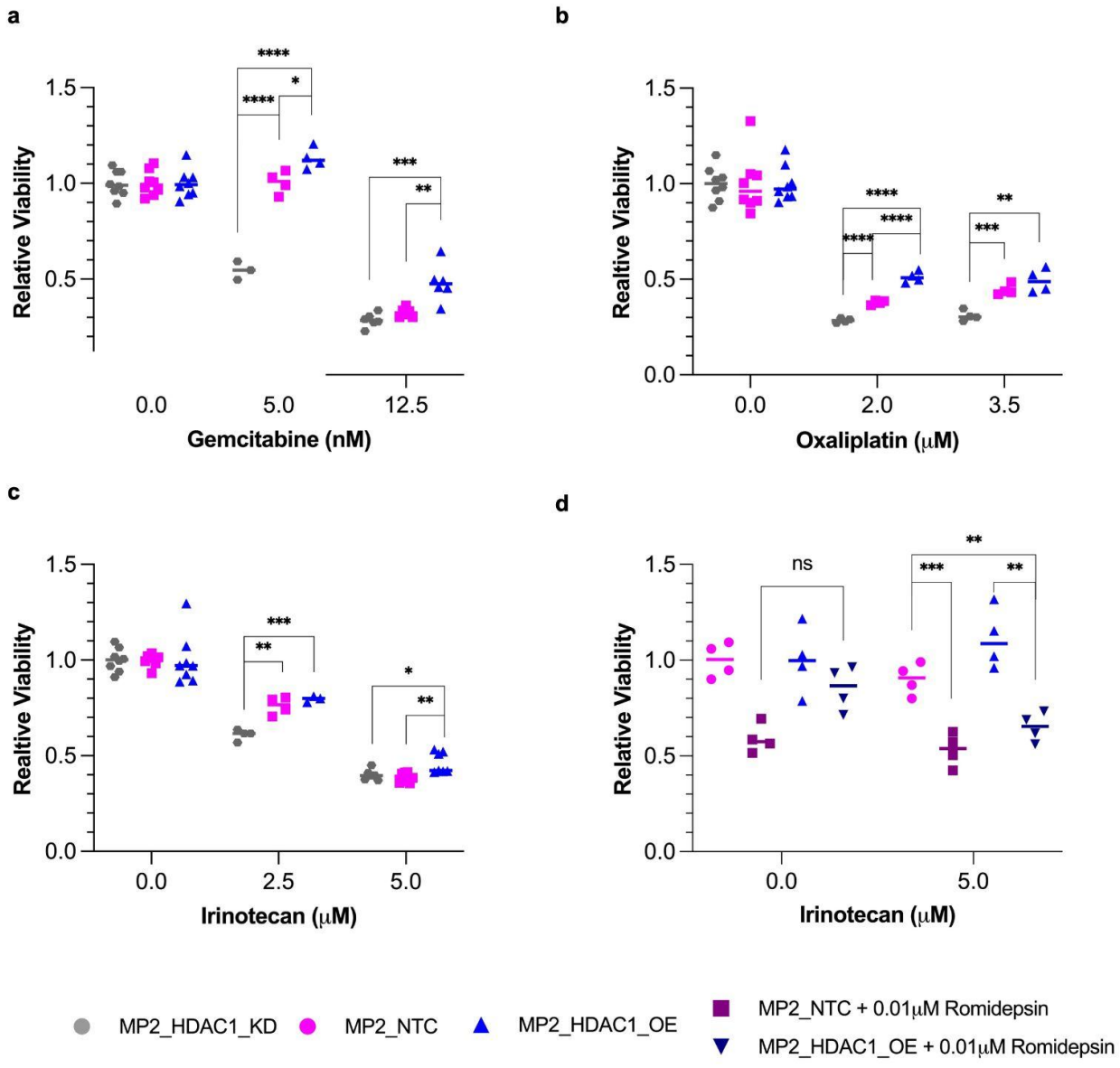

Fig 1. Quantification of cell viability in PDAC cell lines following treatment of chemotherapeutics
Quantification of viability following treatment with **a)** gemcitabine, **b)** oxaliplatin, and **c)** irinotecan in MP2_HDAC1_OE (blue triangles), MP2_NTC (pink squares), and MP2_HDAC1_KD (grey circles) cell lines. The bar represents the median. P-values were calculated using a two-tailed t-test. *p< 0.05, **p< 0.01, ***p<0.001. ns, not significant.
d, Quantification of cell viability following treatment with romidepsin, a HDAC1 inhibitor, in MP2_HDAC1_OE and MP2_NTC cell lines. Bar = median. P-values were calculated using a two-tailed t-test. *p< 0.05, **p< 0.01, ***p<0.001. ns, not significant.

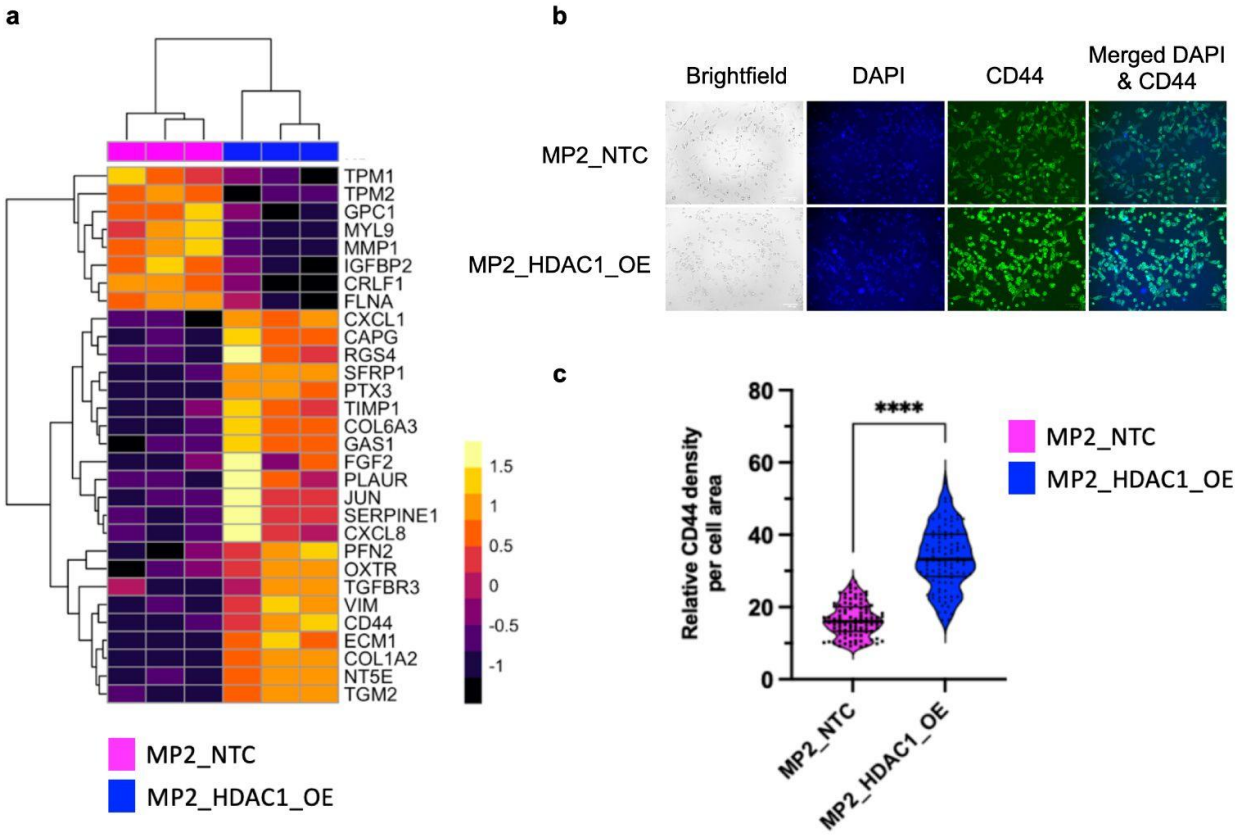

Fig 2. *HDAC1* overexpression is associated with increased expression of EMT genes.
a, Expression of EMT genes in MP2_HDAC1_OE and MP2_NTC cell lines. Each column represents a replicate of the denoted cell line. The color scale denotes the z-score of each gene.
b, Brightfield images and immunofluorescent staining of DAPI (blue), CD44 (green), and merged CD44:DAPI (blue/green) of MP2_HDAC1_OE (bottom) and MP2_NTC (top) cells.
c, Violin plot analysis of immunofluorescent staining of CD44 in MP2_HDAC1_OE (blue) and MP2_NTC cells (pink). 100 cells were measured for each cell line. P-values were calculated using a two-tailed t-test. ****$p<0.0001$.

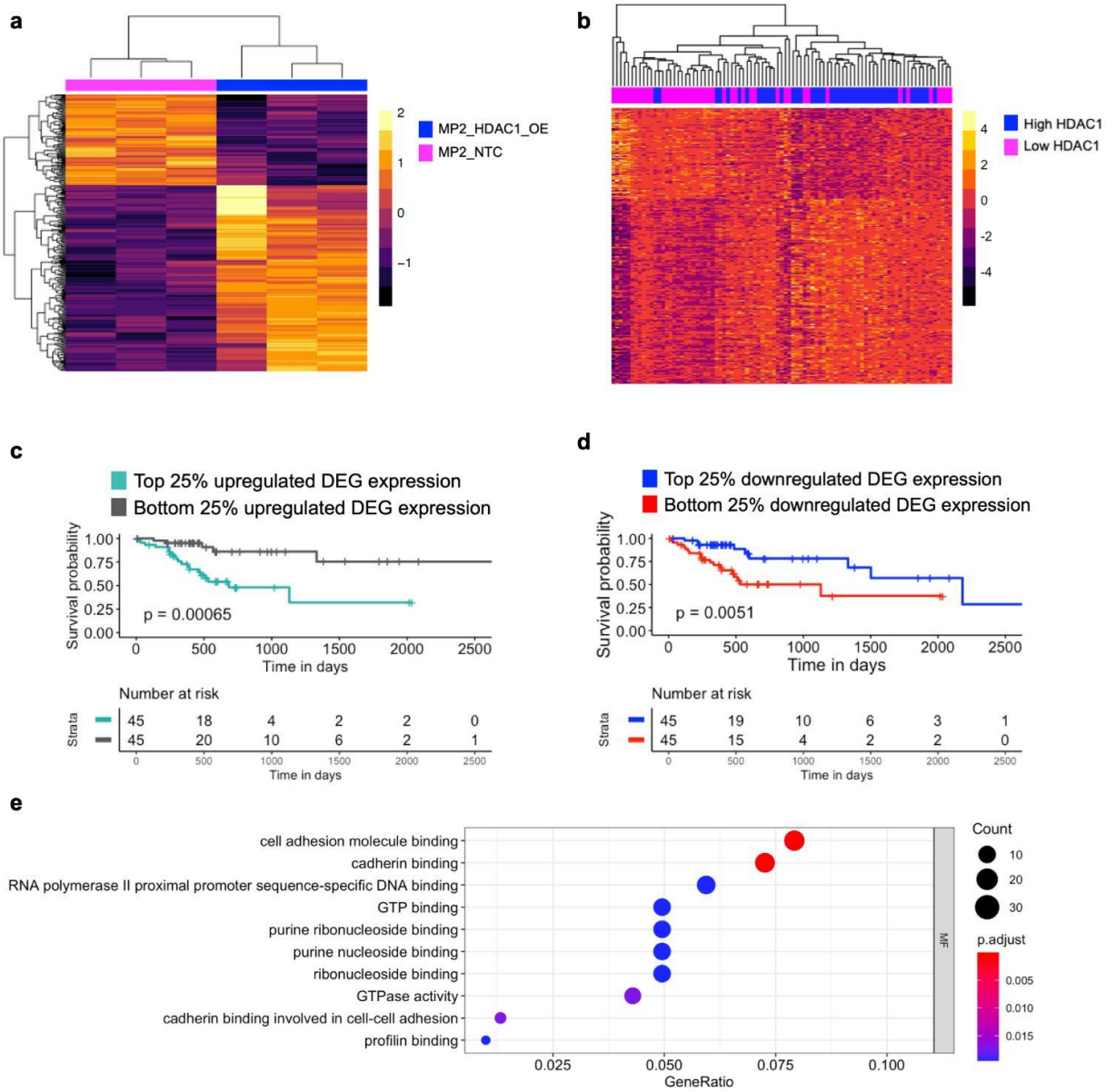

Fig 3. Genes altered by increased *HDAC1* expression in PDAC cell lines and TCGA PDAC samples are associated with patient survival.

a, Expression of DEG in MP2_HDAC1_OE (blue) and MP2_NTC (pink) cell lines. DEG are significantly (padj < 0.1) altered in the same direction in MP2_HDAC1_OE cells and TCGA PDAC tissues with the top 25% of *HDAC1* expression. Each column represents a replicate of the noted cell line. The color scale denotes the z-score of each gene.

b, Expression of DEG in TCGA PDAC samples. Each column represents a tumor sample. The color scale denotes the z-score of each gene. DEG are significantly (padj < 0.1) altered in the same direction in TCGA PDAC tissues with the top 25% of *HDAC1* expression and MP2_HDAC1_OE cells.

c, Overall survival of TCCA PDAC patients (n = 90) with top and bottom 25% of average gene expression of upregulated genes (n = 216) in **a** and **b**. P-values were derived using log-rank test.

d, Overall survival of TCCA PDAC patients (n = 90) with top and bottom 25% of average gene expression of downregulated genes (n = 106) in **a** and **b**. P-values were derived using log-rank test.

e, GO analysis showing enriched molecular functions using the genes (n = 322) in **a** and **b.**

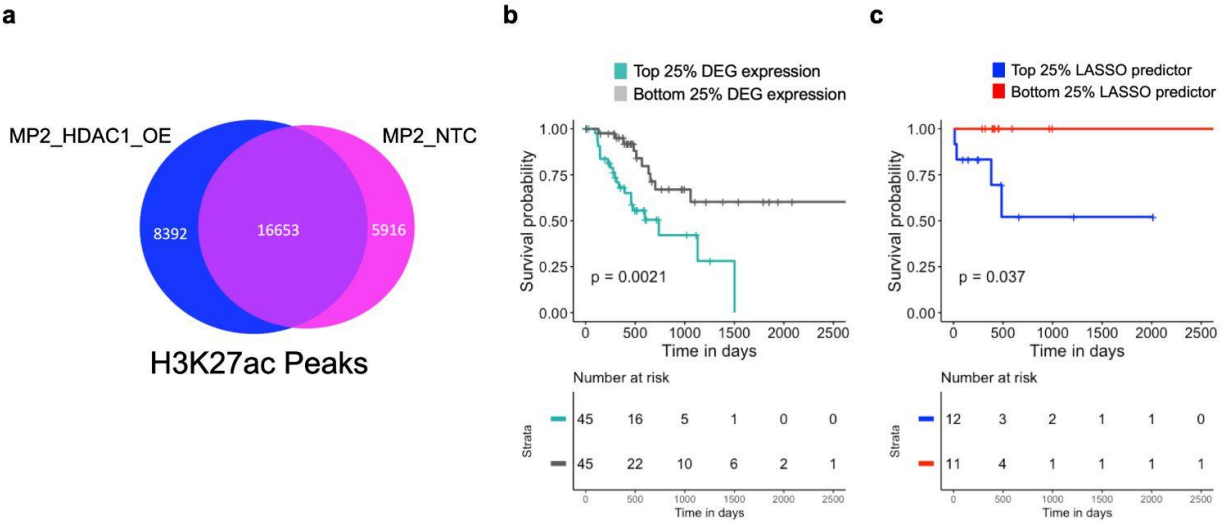

Fig 4. ChIP-sequencing reveals DEG associated with patient survival
a, Venn diagram showing overlap of H3K27ac ChIP-seq peaks in MP2_HDAC1_OE and MP2_NTC cell lines.
b, Overall survival of TCCA PDAC patients (n = 90) with top (teal) and bottom (grey) 25% of average gene expression of upregulated DEG with increased HDAC1 binding and H3K27 acetylation in their promoter upon *HDAC1* overexpression. P-value was derived using log-rank test.
c, Overall survival of TCCA PDAC patients (n = 90) with top (blue) and bottom (red) 25% of predictor values generated from the nine-transcript LASSO model. P-value was derived using log-rank test.

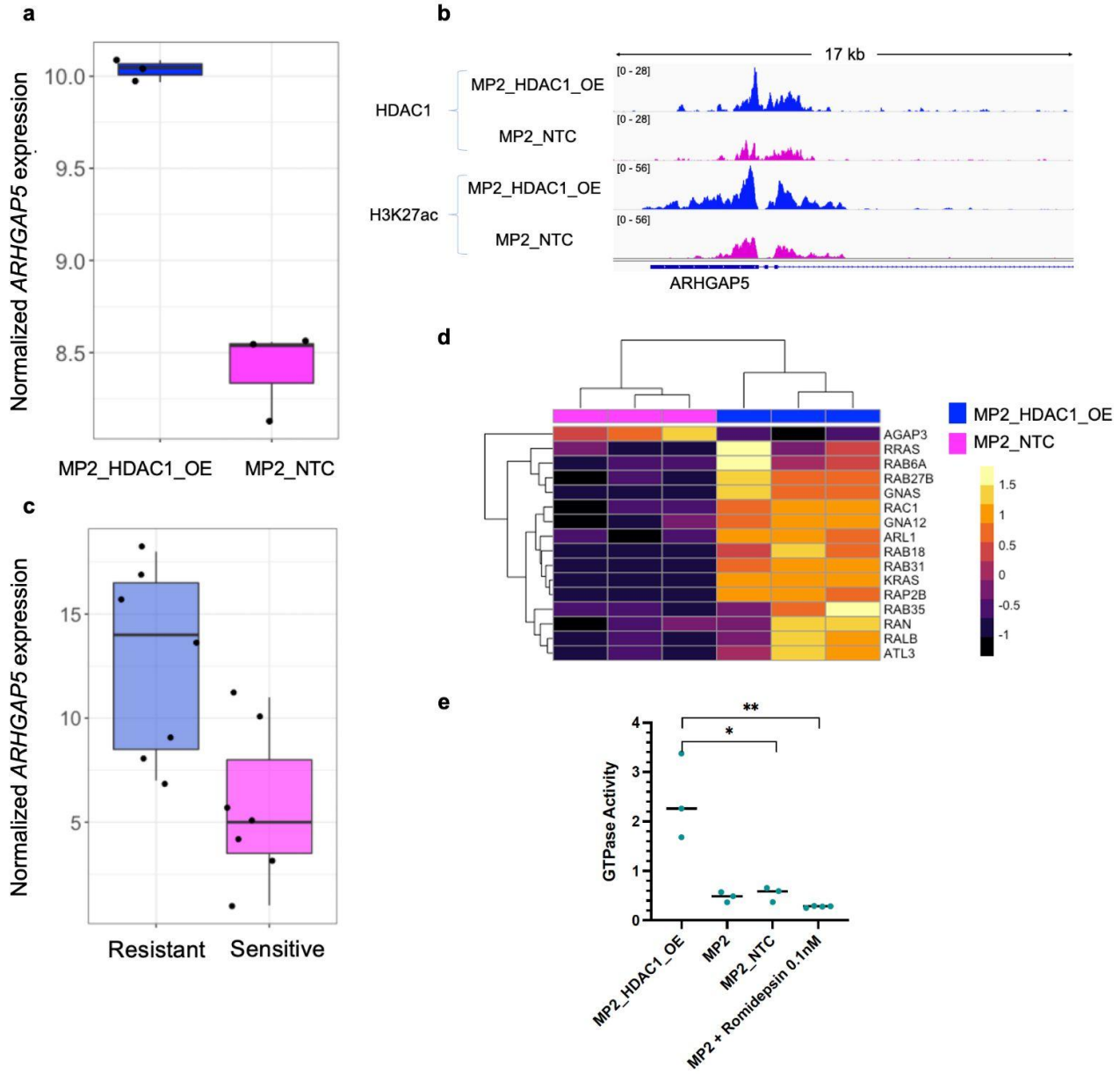

Fig 5. *HDAC1* overexpression is associated with increased GTPase activity.
a, Normalized expression of *ARHGAP5* in MP2_HDAC1_OE (blue) and MP2_NTC (pink) cell lines. The bar is the median. P-values were calculated using an unpaired two-tailed t-test, p = 0.0003479.
b, ChIP-seq analysis of the ARHGAP5 promoter showing increased HDAC1 and H3K27ac peak height in MP2_HDAC1_OE (blue) cells compared to MP2_NTC (pink) cells.
c, Normalized expression of *ARHGAP5* in PDAC cell lines resistant (blue) and sensitive (pink) to gemcitabine. The bar is the median. P-values were calculated using an unpaired two-tailed t-test, p = 0.00831.
d, Expression of DEG involved in GTPase activity in MP2_HDAC1_OE (blue) and MP2_NTC (pink) cell lines. Each column represents a replicate of the noted cell line. The color scale denotes the z-score of each gene.
e, Comparison of GTPase activity in the following cell lines: MP2_HDAC1_OE, MP2, MP2_NTC, and MP2 treated with romidepsin. P-values were calculated using a two-tailed t-test. *p< 0.05, **p< 0.01.